Simple Template-Free Solution Route for the Controlled Synthesis of $Cu(OH)_2$ and CuO Nanostructures

Conghua Lu, Limin Qi,* Jinhu Yang, Dayong Zhang, Nianzu Wu, and Jiming Ma

State Key Laboratory for Structural Chemistry of Unstable and Stable Species, College of Chemistry, Peking University, Beijing, 100871, People's Republic of China

Received: July 21, 2004; In Final Form: August 29, 2004

The controlled synthesis of $Cu(OH)_2$ nanowires and nanoribbons in a solution phase has been realized with high yield at low cost by simply dropping KOH and ammonia solutions into an aqueous solution of $CuSO_4$ at ambient temperature. It is demonstrated that the morphology of nanostructured $Cu(OH)_2$ is significantly influenced by the feeding manner of the alkaline solutions. A rational mechanism based on coordination self-assembly and oriented attachment is proposed for the selective formation of the polycrystalline $Cu(OH)_2$ nanowires and single-crystalline $Cu(OH)_2$ nanoribbons. In the presence of a polymeric additive, poly(acrylic acid) (PAA), ordered assemblies of $Cu(OH)_2$ nanorods can be readily obtained. Furthermore, well-defined CuO nanostructures, such as CuO nanoplatelets, nanoleaflets, and nanowires, were produced by thermal dehydration of the as-prepared $Cu(OH)_2$ nanostructures in solution or in the solid state. Scanning electron microscopy (SEM), transmission electron microscopy (TEM), high-resolution TEM (HRTEM), X-ray diffraction (XRD), and X-ray photoelectron spectroscopy (XPS) were used to characterize the products.

Introduction

One-dimensional (1D) nanostructured materials, such as nanotubes, nanorods/nanowires, and nanobelts/nanoribbons, have attracted considerable attention due to their fundamental importance and potential wide-ranging applications.[1] Among the various methods developed for the fabrication of 1D nanomaterials, the solution-phase chemical synthesis has been considered as the most promising route in terms of cost, throughput, and the potential for large-scale production.[2] Generally, the solution-phase chemical approach may be classified into the template method, which employs hard[3] and soft[4−6] templates, and the template-free method, which uses surface-capping reagents for anisotropic confinements[7] or directly utilizes the highly anisotropic crystal structure of solid materials without capping reagents.[8] Accompanying the advance in synthesis method of 1D nanostructures, there is growing interest in the morphological control of the 1D nanostructures. In particular, as a new family of 1D nanostructures, nanobelts/nanoribbons are receiving increasing attention because of their unique properties and potential applications in building functional nanodevices;[9] however, there are few reports concerning the wet chemical fabrication of inorganic nanobelts.[10−12] It remains a significant challenge to realize elaborate control of the morphology of 1D nanostructures in the absence of template in aqueous solution.

As well-known layered materials, $Cu(OH)_2$ and basic Cu(II) salts with an orthorhombic structure have received much attention in recent years.[12−18] Since its magnetic properties are sensitive to the intercalation of molecular anions, $Cu(OH)_2$ has the potential application as sensors.[13] Orthorhombic $Cu_2(OH)_3Cl$ was recently found in living organisms as the first identified copper-based biomineral, which is formed in the teeth of a carnivorous marine worm and exists as polycrystalline nanofibers arranged along the outer contour of the tooth tip, leading to an extraordinary resistance to abrasion.[14] Recently, 1D $Cu(OH)_2$ nanomaterials have been fabricated through solution-phase chemical approaches involving coordination self-assembly. For example, polycrystalline $Cu(OH)_2$ nanoribbons were prepared in aqueous solution of ammonia using Cu_2S nanowires as precursors,[12a] whereas single-crystalline $Cu(OH)_2$ nanoribbon[12b] and nanotube[16] arrays were prepared by surface oxidation of copper foil in alkaline solutions. On the other hand, polycrystalline $Cu(OH)_2$ nanowires were synthesized by a simple two-step process in aqueous ammonia and NaOH solutions[17] or by the interaction between a copper complex and NaOH at the aqueous−organic interface.[18] However, it is noted that the effective adjustment of 1D $Cu(OH)_2$ nanostructures between ribbon- and wirelike morphologies in one synthesis system has not been achieved so far.

As a p-type semiconductor with a narrow band gap (1.2 eV), CuO has been widely exploited for diverse applications as heterogeneous catalysts,[19] gas sensors,[20] lithium ion electrode materials,[21] and field emission (FE) emitters.[22] Many recent efforts have been directed toward the fabrication of nanostructured CuO to enhance its performance in currently existing applications. In particular, a variety of 1D CuO nanostructures have been prepared by high-temperature approaches[23] and low-temperature wet chemical approaches.[21,24] Notably, 1D $Cu(OH)_2$ nanostructures have been frequently employed as the precursors for the fabrication of 1D CuO nanostructures.[12b,18,25] However, a detailed study on the transformation from $Cu(OH)_2$ to CuO nanostructures is still lacking.

In this work, wire- and ribbonlike $Cu(OH)_2$ nanostructures have been selectively prepared by a two-step, template-free, wet chemical approach just through simply changing the feeding order of two alkaline solutions. The transformation from the 1D $Cu(OH)_2$ nanostructures to a variety of novel CuO nanostructures (wires, platelets, leaflets, and flowers) has been

* To whom correspondence should be addressed. E-mail: liminqi@chem.pku.edu.cn.

10.1021/jp046772p CCC: $27.50
Published on Web 10/21/2004

realized by thermal dehydration of the as-prepared $Cu(OH)_2$ nanostructures either in solution or in the solid state.

Experimental Section

Synthesis of $Cu(OH)_2$ Nanostructures. Two different methods were used for the two-step synthesis of $Cu(OH)_2$ nanostructures, i.e., the KOH/NH_3 route and the NH_3/KOH route. In a typical KOH/NH_3 route to $Cu(OH)_2$ nanostructures, 0.8 mL of 1 M KOH solution was first dropped into 2 mL of 0.1 M $CuSO_4$ solution under rigorous stirring at ambient temperature (~19 °C), which was followed by the dropping of 0.3 mL of ammonia solution (12.5 wt %, ~7.0 M). After 3 min of further stirring, the mixed solution was kept static in a sealed vessel for 12 h (unless otherwise stated). The resultant precipitate was filtered off, washed thoroughly with deionized water, and dried in a vacuum at 25 °C for 12 h. For the NH_3/KOH route to $Cu(OH)_2$ nanostructures, the synthesis procedure was identical to that for the KOH/NH_3 route except for the feeding order of the two alkaline solutions; i.e., the KOH solution was added after the addition of the ammonia solution. Occasionally, a polymeric additive, poly(acrylic acid) (PAA, Aldrich, M_n = 5100), was added to the solution before the addition of the alkaline solutions for the investigation of its effect on the $Cu(OH)_2$ nanostructures.

Transformation of $Cu(OH)_2$ Nanostructures into CuO Nanostructures. For the dehydration of $Cu(OH)_2$ nanostructures in solution, the $Cu(OH)_2$ nanostructures formed immediately after adding both alkaline solutions were heated at a given temperature (e.g., 30 and 50 °C)for 12 h; alternatively, the as-prepared $Cu(OH)_2$ nanostructures were separated and redispersed in deionized water, followed by heat treatment at 70 °C for a given time (e.g., 1 and 12 h). For the dehydration of $Cu(OH)_2$ nanostructures in the solid state, the as-prepared $Cu(OH)_2$ nanostructures were heated at 120 °C for 2 h to dehydrate and subsequently at 180 °C for another 3 h to promote crystallization.

Characterization. Field-emission scanning electron microscopy (FE-SEM) images were taken on a FEI STRATA DB235 microscope at an accelerating voltage of 10 kV. X-ray diffraction (XRD) was carried out on a Rigaku Dmax-2000 X-ray diffractometer equipped with Cu Kα radiation. Transmission electron microscopy (TEM) was performed on a JEOL JEM-200CX microscope with an accelerating voltage of 160 kV. High-resolution TEM (HRTEM) was performed on a Hitachi 9000HAR microscope. Selected samples were also investigated by X-ray photoelectron spectroscopy (XPS, Kratos Axis Ultra spectrometer) with Al Kα monochromatized X-ray source running at 250 W and the base pressure in the analytic chamber about 5×10^{-9} Torr.

Results and Discussion

Synthesis of $Cu(OH)_2$ Nanostructures. The synthesis of $Cu(OH)_2$ nanostructures was simply achieved by successively dropping KOH and ammonia solutions into an aqueous solution of $CuSO_4$ at ambient temperature (~19 °C). According to the feeding order of the two alkaline solutions, two different synthesis routes were adopted: the KOH/NH_3 route where KOH was added first and ammonia was added subsequently, and the NH_3/KOH route where ammonia was added first followed by the addition of KOH. Figure 1 shows typical SEM and TEM images of the as-prepared $Cu(OH)_2$ nanostructures produced via the KOH/NH_3 route and aged for 12 h. The product consists entirely of very long (~20 μm) wirelike nanostructures (Figure 1a), and it appears that the nanowires tend to assemble into

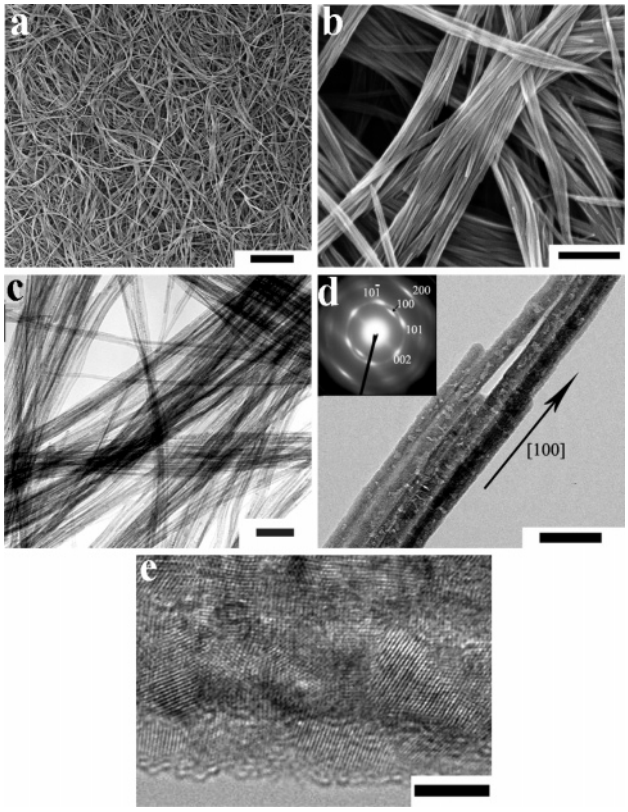

Figure 1. SEM (a, b), TEM (c, d), and HRTEM (e) images of $Cu(OH)_2$ nanowires prepared via the KOH/NH_3 route aged for 12 h. Inset shows ED pattern of the bundled nanowires. Scale bars: (a) 5 μm; (b) 500 nm; (c) 100 nm; (d) 50 nm; (e) 5 nm.

nanowire bundles up to several hundreds of nanometers in diameters (Figure 1b). The TEM images (Figure 1c,d) suggest that the 1D nanostructures exhibit relatively uniform width (~10 nm), which is consistent with a cylindrical wirelike morphology rather than a ribbonlike morphology. The HRTEM image (Figure 1e) suggests that the nanowires are polycrystalline nanowires consisting of orthorhombic $Cu(OH)_2$ nanocrystallites. However, the electron diffraction (ED) pattern corresponding to a bundle of nanowires shows some diffusive, yet strong, reflections, agreeing well with the orthorhombic structure of $Cu(OH)_2$, which suggests that orientations of the crystallites are not random but coordinated with the [100] direction being the preferential growth direction of the polycrystalline nanowires or the growth direction on average. The XRD pattern of the nanowires aged for 12 h is presented in Figure 2, which shows sharp diffraction peaks attributed to the orthorhombic $Cu(OH)_2$, implying the formation of pure $Cu(OH)_2$ nanowires. It is noted that only (0*kl*) reflections are clearly observed, which is in good agreement with the $Cu(OH)_2$ nanowires with preferential orientation along the [100] direction. The polycrystalline $Cu(OH)_2$ nanowires with preferential orientation could form through an oriented attachment mechanism,[26] which is reminiscent of the polycrystalline, [100]-oriented $Cu(OH)_2$ nanoribbons obtained in aqueous solution by using Cu_2S nanowires as precursors.[12a]

To understand the growth process of the $Cu(OH)_2$ nanowires in solution, we investigated the effect of aging time on the product. It was observed that the solution precipitated immediately after the addition of the KOH solution. As shown in Figure 2, the XRD pattern of the obtained precipitates suggests the precipitates consist of triclinic $Cu(OH)_2 \cdot H_2O$ crystals (JCPDS 42-0746). The XRD patterns of the products obtained at different aging time after the addition of the ammonia solution

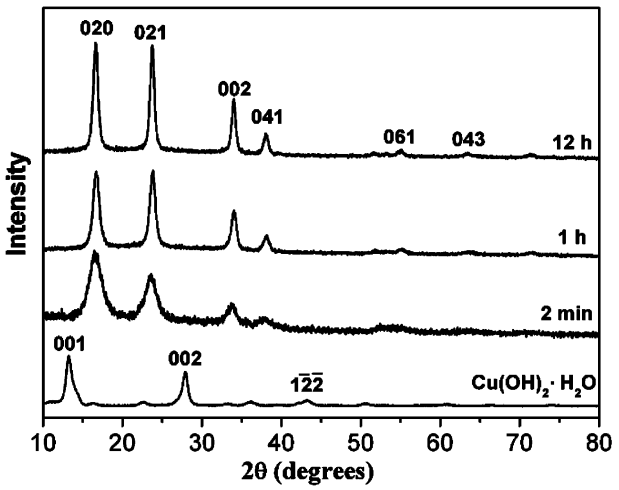

Figure 2. XRD patterns of $Cu(OH)_2$ nanowires prepared via the KOH/NH_3 route aged for different periods. XRD pattern of $Cu(OH)_2 \cdot H_2O$ precipitates obtained before adding ammonia is also displayed.

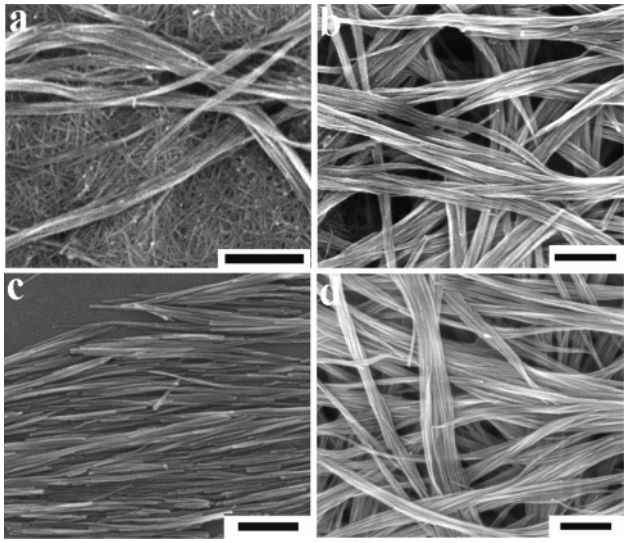

Figure 3. SEM images of $Cu(OH)_2$ nanowires prepared via the KOH/NH_3 route aged for 2 min (a) and 1 h (b), and the $Cu(OH)_2$ nanowires obtained via the KOH/NH_3 route aged for 1 h (c) and 12 h (d) and sonicated for 10 min. Scale bars: 500 nm.

are also shown in Figure 2. After 2 min of aging, the product shows the XRD pattern corresponding to pure orthorhombic $Cu(OH)_2$, indicating a quick transformation from $Cu(OH)_2 \cdot H_2O$ to $Cu(OH)_2$ accompanying the addition of ammonia. The relatively broader diffraction peaks suggests the smaller crystallite size for the nanowires formed at the early stage. The typical SEM image of the sample is presented in Figure 3a, which shows that a large number of separated nanowires ~10 nm in diameter coexisted with some bundles of nanowires (larger than 50 nm in bundle diameter). At an aging time of 1 h, the diffraction peaks were considerably narrowed, suggesting an increase in the crystallite size. Meanwhile, all the individual nanowires were assembled into bundles (Figure 3b), which is very similar to the product obtained after 12 h of aging (Figure 1a,b). However, simple ultrasonic treatment using a normal ultrasonic bath revealed a considerable difference in the toughness between the nanowires aged for 1 and 12 h. Upon 10 min of sonication, most of the long nanowires aged for 1 h were broken into short nanorods around 200−500 nm in length (Figure 3c). In contrast, the long nanowires aged for 12 h were not broken at all upon 10 min of sonication and the original

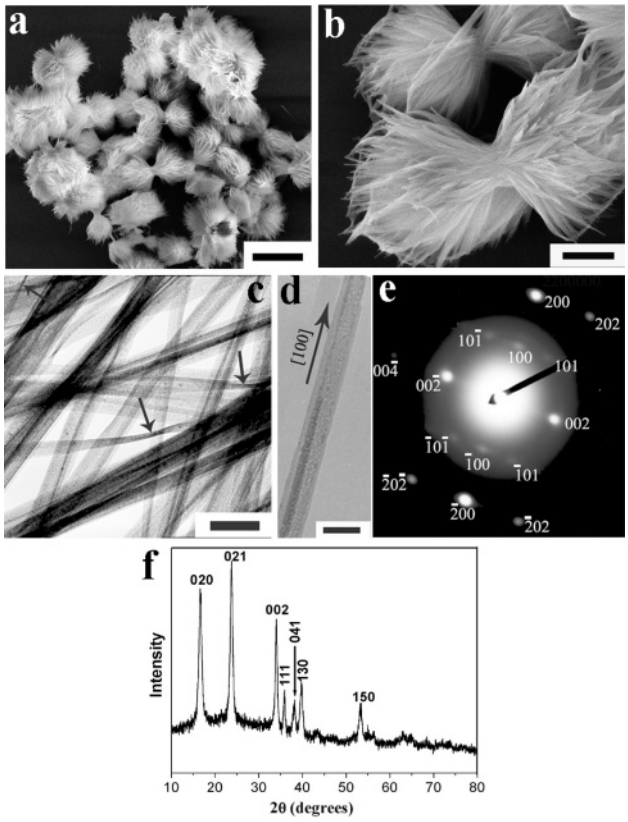

Figure 4. SEM (a, b) and TEM (c, d) images and ED (e) and XRD (f) patterns of $Cu(OH)_2$ nanoribbons prepared via the NH_3/KOH route. The ED pattern shown in plate e corresponds to the single nanoribbon shown in plate d. Scale bars: (a) 5 μm; (b) 1 μm; (c) 200 nm; (d) 100 nm.

morphology was almost completely reserved (Figure 3d). This result suggests that the nanowires aged for 1 h were still not well-crystallized and continued to develop into the well-crystallized nanowires probably through the Ostwald ripening process, which has been believed to assist the 1D growth process by oriented attachment.[26c] It is worth noting that oriented arrays of polycrystalline $Cu_2(OH)_3Cl$ nanofibers play a key role in enhancing hardness and stiffness of the teeth of a marine worm.[14] Therefore, the current room-temperature solution synthesis of bundles of polycrystalline $Cu(OH)_2$ nanowires, which has a similar orthorhombic structure, would have relevant biological implications.

When the feeding order of the two alkaline solutions was altered, a significant change in the morphology of the produced 1D $Cu(OH)_2$ nanostructures occurred. Figure 4 presents typical SEM and TEM images of the as-prepared $Cu(OH)_2$ nanostructures produced via the NH_3/KOH route along with their ED and XRD patterns. The SEM images (Figure 4a,b) suggest that the product consists of well-defined sheaves of nanoribbons about 5 μm in length, and the TEM image (Figure 4c) shows thinning in the smooth bend and wring sections indicated by the arrows, which is characteristic of ribbonlike nanostructures. The nanoribbons are typically 30−100 nm in width and several nanometers in thickness. An enlarged TEM image showing a single nanoribbon is presented in Figure 4d with its related ED pattern shown in Figure 4e, which clearly shows spots associated with the [010] zone axis of the orthorhombic $Cu(OH)_2$, indicating that the nanoribbon is a single-crystal grown along the [100] direction and enclosed with the (010) and the (001) as the top and side planes, respectively. The related X-ray diffraction pattern (Figure 4f) suggests the nanoribbons consist

SCHEME 1: Schematic Illustration of the Growth Process of 1D $Cu(OH)_2$ Nanostructures in Solution

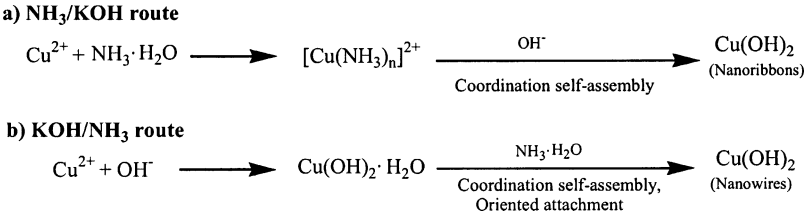

of pure orthorhombic $Cu(OH)_2$ and the presence of reflections other than the (0*kl*) reflections can be rationalized by considering that the nanoribbons are not well-aligned parallel to the substrate as they aggregate into sheaflike assemblies. The obtained [100]-oriented $Cu(OH)_2$ nanoribbons are reminiscent of the single-crystalline $Cu(OH)_2$ nanoribbons prepared by surface oxidation of copper foil in ammonia solutions where $Cu(OH)_2$ nanoribbons were grown almost vertically on the copper surface to form nanoribbon arrays.[12b] To the best of our knowledge, this is the first realization of selective synthesis of $Cu(OH)_2$ nanowires and nanoribbons in an aqueous solution system through simple alteration of the feeding order of two alkaline solutions. It is noteworthy that for the current NH_3/KOH route to the $Cu(OH)_2$ nanoribbons, a considerable excess of ammonia with respect to $CuSO_4$ (e.g., $[NH_3]/[CuSO_4] \sim 10$) was required; otherwise, $Cu(OH)_2$ nanowires may be formed. For example, it was reported that only $Cu(OH)_2$ nanowires were obtained at a relatively low ammonia concentration ($[NH_3]/[CuSO_4] \sim 1$) when a similar NH_3/NaOH route was employed.[17]

The exact mechanism for the selective formation of $Cu(OH)_2$ nanowires and nanoribbons remains to be investigated in more detail. As is well-known, the orthorhombic $Cu(OH)_2$ with a layered structure parallel to (010) consists of olated >Cu-$(OH)_2$Cu< chains oriented along [100] and characterized by the square-planar coordination of the Cu^{2+} ions by OH^- ions with strong σ_{x2-y2} bonds. According to the Bravais−Donnay−Harker law, the growth of $Cu(OH)_2$ along [100] is much faster than along other directions and the [010] direction is the lowest growth direction, leading to a tendency to form a ribbonlike structure.[12,16] Based on the recently discussed coordination self-assembly mechanism for the formation of $Cu(OH)_2$ nanoribbons, a tentative mechanism (Scheme 1) involving coordination self-assembly and oriented attachment was proposed for the formation of the current 1D $Cu(OH)_2$ nanostructures. For the NH_3/KOH route to $Cu(OH)_2$ nanostructures, a homogeneous $[Cu(NH_3)_n]^{2+}$ solution was formed during the first step. Upon adding the KOH solution, OH^- replaced NH_3 in the $[Cu(NH_3)_n]^{2+}$ complex to form square-planar $[Cu(OH)_4]^{2-}$ units and a coordination self-assembly of the >$Cu(OH)_2$Cu< chains occurred quickly, resulting in the formation of single-crystalline $Cu(OH)_2$ nanoribbons. The nucleation of $Cu(OH)_2$ could start from localized regions with relatively high $[Cu(NH_3)_n]^{2+}$ concentrations. Once the nuclei were formed, the growth of Cu-$(OH)_2$ nanoribbons started on it, leading to the formation of sheaves of nanoribbons. The complex of $[Cu(NH_3)_n]^{2+}$ may act as a molecular transporter that transports Cu^{2+} to the growing nanoribbon tips with OH^- ligands attached; moreover, NH_3 may probably adsorb on the (010) surface to further slow the growth along the [010] direction, favoring the formation of the ribbonlike structure. When the feeding order of the NH_3 and KOH solutions was altered, i.e., the KOH/NH_3 route was employed, $Cu(OH)_2 \cdot H_2O$ precipitated during the first step. Upon adding the ammonia solution, the $Cu(OH)_2 \cdot H_2O$ precipitate was converted to $Cu(OH)_2$ crystals, probably through a solid−liquid−solid (SLS) process where the complex $[Cu(NH_3)_n]^{2+}$ may also play an important role as a transporter. Although there was still a tendency to form $Cu(OH)_2$ nanoribbons by coordination self-assembly, during the SLS process, the $[Cu(NH_3)_n]^{2+}$ concentration in the solution could be relatively lower, which did not favor the formation of nuclei for the $Cu(OH)_2$ nanoribbons. Therefore, individual $Cu(OH)_2$ nanoparticles rather than long $Cu(OH)_2$ nanoribbons were formed at the beginning. Then $Cu(OH)_2$ nanowires grew preferentially along the [100] direction by the oriented attachment of the primary nanoparticles, which was coupled with coordination self-assembly, resulting in polycrystalline $Cu(OH)_2$ nanowires. The individual nanowires were further attached side by side to assemble into bundles on further aging, accompanying an Ostwald ripening process leading to larger crystallite sizes and tougher nanowires. The obtained nanowire bundle structures are reminiscent of the bundles of $BaSO_4/BaCrO_4$ nanofibers obtained in the presence of polymeric additives;[7d,e] however, the current nanowire bundles were produced in polymer-free processes, and the driving force could partly come from the lateral capillary forces. On the other hand, the nanobelt bundles obtained via the NH_3/KOH route may be formed due to the growth from the central nucleation points, which is somewhat similar to the bundles of $BaSO_4/BaCrO_4$ nanofibers formed by growth from individual nucleation points under the direction of polymers.[7d,e]

Although the NH_3/KOH route seems to be favorable for the formation of $Cu(OH)_2$ nanoribbons, such a tendency can be restrained by polymeric additives present in the solution. Poly-(acrylic acid) (PAA) is a typical crystal growth inhibitor for many inorganic minerals.[27] When 2.5×10^{-4} M PAA was present in the $CuSO_4$ solution before the addition of the two alkaline solutions, the product obtained by the NH_3/KOH route consisted of relatively uniform assemblies of parallel-aligned $Cu(OH)_2$ nanorods 5−10 nm in width and ~200 nm in length (Figure 5a,b). From the HRTEM image (Figure 5c), it is observed that the nanorod is a single-crystal grown along the [100] direction, the fastest growth direction of the orthorhombic $Cu(OH)_2$. The amorphous area can be observed on both sides of the nanorod, implying the adsorption of the polymer molecules on the nanorod. The corresponding XRD pattern (Figure 5d) is indicative of orthorhombic $Cu(OH)_2$, confirming the formation of $Cu(OH)_2$ nanorod assemblies. The XPS result (Figure 6) shows typical Cu $2p_{3/2}$ and Cu $2p_{1/2}$ peaks with the measured binding energy of 934.5 and 954.2 eV, respectively, as well as their concomitant shake-up lines at 942.4 and 962.4 eV, which is indicative of the paramagnetic chemical state of Cu^{2+};[28] moreover, the well-resolved C 1s peak is observed at 284.8 eV, confirming the presence of PAA within the assemblies, i.e., the formation of PAA/$Cu(OH)_2$ hybrid nanomaterials. It is therefore reasonable to believe that the adsorption of PAA modifies the growth rate for special crystal planes to some extent. Especially, it could restrain the preferential growth along the [001] direction with respect to the [010] direction, resulting in the formation of $Cu(OH)_2$ nanorods rather than nanoribbons. The presence of adsorbed PAA molecules may also be contributed to the parallel attachment of the short

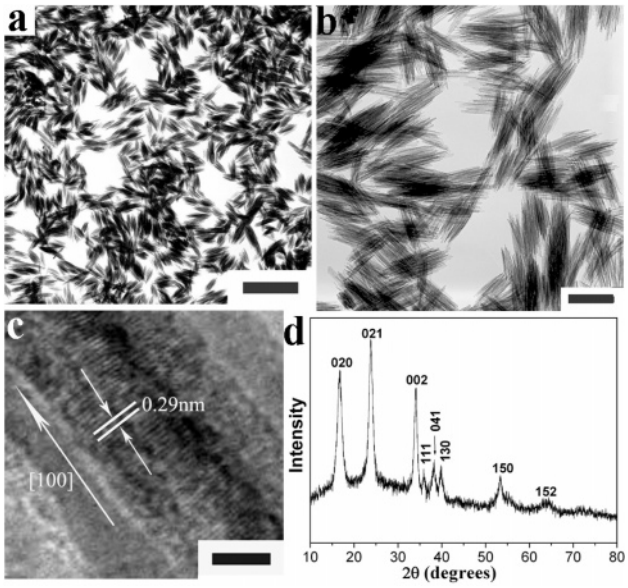

Figure 5. TEM (a, b) and HRTEM (c) images and the XRD pattern (d) of $Cu(OH)_2$ nanorod assemblies prepared via the NH_3/KOH route in the presence of PAA. Scale bars: (a) 1 μm; (b) 200 nm; (c) 3 nm.

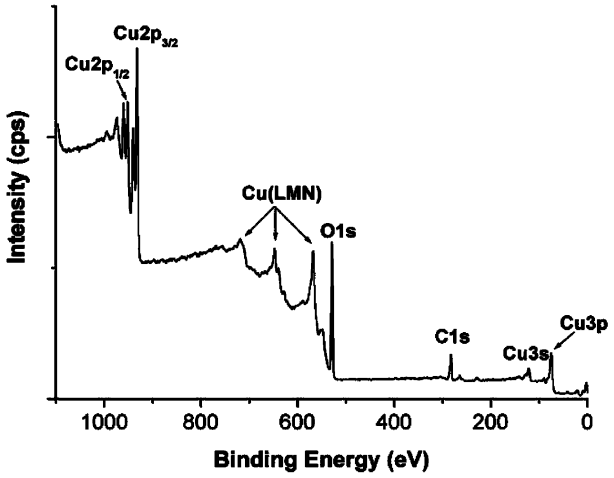

Figure 6. X-ray photoelectron spectrum of $Cu(OH)_2$ nanorod assemblies prepared via the NH_3/KOH route in the presence of PAA.

nanorods, which leads to the formation of the novel assemblies of $Cu(OH)_2$ nanorods. Such $Cu(OH)_2$-based organic−inorganic hybrids with ordered nanostructures would find potential application as ferromagnets.[29] It is worth mentioning that the $Cu(OH)_2$ product obtained by the KOH/NH_3 route in the presence of PAA still exhibited bundles of nanowires, suggesting that PAA would be favorable for the formation of cylindrical 1D nanostructures.

Synthesis of CuO Nanostructures. It is well-known that orthorhombic $Cu(OH)_2$ can be easily transformed to monoclinic CuO upon heat treatment. The thermal dehydration of the obtained 1D $Cu(OH)_2$ nanostructures in the solution phase and in the solid state was investigated but special effort was devoted to the transformation in solution as the transformation of $Cu(OH)_2$ nanoribbons to CuO nanoribbons/nanowires in solid state has been well-documented.[12b,25] When the $Cu(OH)_2$ nanowires obtained by the KOH/NH_3 route were heated in the original solution immediately after the addition of the two alkaline solutions, a complete transformation to CuO occurred at a temperature as low as 50 °C. As shown in Figure 7a, some nanoplatelets showing irregular contours appeared in addition to the bundles of $Cu(OH)_2$ nanowires after being aged for 12 h

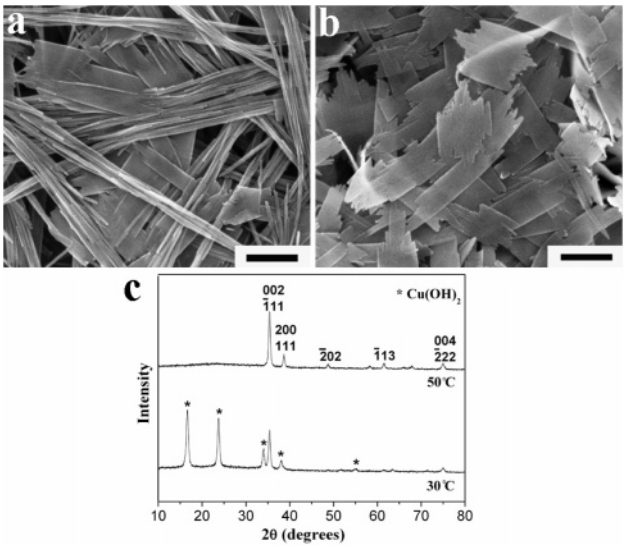

Figure 7. SEM images (a, b) and XRD patterns (c) of CuO nanoplatelets obtained by thermal dehydration of the $Cu(OH)_2$ nanowires prepared via the KOH/NH_3 route immediately after the addition of the KOH and ammonia solutions: (a) 30 °C; (b) 50 °C. Scale bars: 500 nm.

at 30 °C. The corresponding XRD pattern (Figure 7c) shows the appearance of reflections attributed to monoclinic CuO, suggesting the part transformation of $Cu(OH)_2$ to CuO. When aged at 50 °C, the $Cu(OH)_2$ nanowires were completely converted to the irregular CuO nanoplatelets (Figure 7b), which was confirmed by the corresponding XRD pattern (Figure 7c).

If the well-developed $Cu(OH)_2$ nanowires after 12 h of aging were separated and redispersed in water, the temperature for a complete transformation to CuO within 12 h was increased to ∼70 °C. Figure 8 shows typical TEM and HRTEM images as well as the XRD pattern of the products dehydrated at 70 °C for different times. When heated for 1 h, rhombic, leafletlike nanostrips appeared in addition to the original bundles of $Cu(OH)_2$ nanowires accompanying the appearance of the XRD peaks characteristic of monoclinic CuO; after 12 h of heating, uniform nanoleaflets 0.7−0.8 μm in length, ∼250 nm in width, and ∼50 nm in thickness were obtained, and the corresponding XRD pattern suggests that the product consists of pure monoclinic CuO. This result suggests a gradual transformation of the $Cu(OH)_2$ nanowire bundles to the CuO nanoleaflets with heating at 70 °C. The ED pattern of a single CuO nanoleaflet shows spots due to the [001] zone axis of monoclinic CuO, indicating that the CuO nanoleaflet is a single crystal elongated along the [010] direction with the top surface of the (001) plane, which is supported by the related HRTEM image.

It is noted that Matijević et al. have prepared polycrystalline ellipsoidal CuO colloids by a controlled double-jet precipitation technique using NaOH and $Cu(NO_3)_2$ as the reactants, and they believed that the polycrystalline CuO ellipsoids were formed by aggregation of primary CuO nanoparticles.[24a] Recently, Zeng et al. have prepared hierarchical dandelion-like architectures constructed with single-crystalline rhombic CuO nanostrips as building units through a hydrothermal synthesis in alkaline ethanol solution, and they proposed that the CuO nanostrips (larger than 600 nm in breadth) were formed by oriented attachment of CuO nanoribbons (about 10−20 nm in breadth).[24d] It should be pointed out that during the solution synthesis of CuO, the final product composition and morphology are largely dependent on the synthesis condition, such as basicity and solvent, and the solid precursors including $Cu(OH)_2$ may exist only momentarily or may not exist at all. In the current situation,

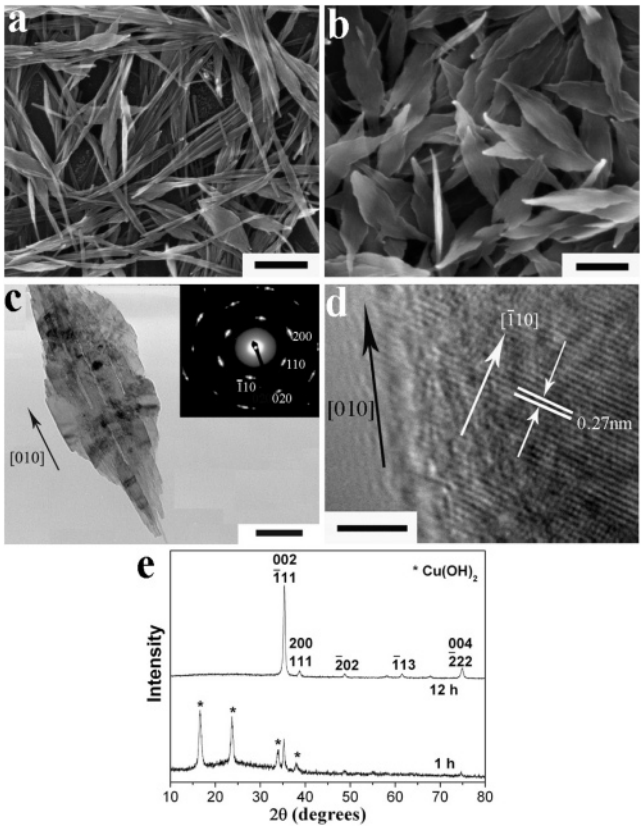

Figure 8. SEM (a, b), TEM (c), and HRTEM (d) images and XRD patterns (e) of CuO nanoleaflets obtained by thermal dehydration of the as-prepared $Cu(OH)_2$ nanowires in water at 70 °C for different times: (a) 1 h; (b−d) 12 h. Inset shows ED pattern of the single CuO nanoleaflet. Scale bars: (a, b) 500 nm; (c) 100 nm; (d) 3 nm.

the CuO nanoleaflets may form by a reconstructive transformation from $Cu(OH)_2$ in aqueous solution involving a dissolution reaction followed by the crystallization of CuO.[30] It is noteworthy that at the early stage of the transformation, the intermediate state of transformation can be observed, which indicates that the CuO nanoleaflets were grown from some parts of the $Cu(OH)_2$ nanowires (Figure 8a). Moreover, when the transformation was complete, some parallel linear traces on the CuO nanoleaflets due to the sacrificial precursors of $Cu(OH)_2$ nanowire bundles can be clearly observed (Figure 8c). Therefore, it can be reasonably proposed that upon heating in water, some parts of the $Cu(OH)_2$ nanowires were preferentially dissolved and then CuO nucleated on some parts of the undissolved $Cu(OH)_2$ nanowires, which was followed by the gradual growth of CuO nanoleaflets accompanying the dissolution of the $Cu(OH)_2$ nanowires, both the bare nanowires and the nanowires encapsulated within the CuO nanoleaflets.

For comparison purpose, the thermal dehydration of the sheaves of $Cu(OH)_2$ nanoribbons, which were obtained by the NH_3/KOH route, in solution was also investigated. As shown in Figure 9, unique, flowerlike aggregates consisting of CuO nanopetals were obtained after the as-prepared $Cu(OH)_2$ nanoribbons were redispersed in water and heated at 70 °C for 12 h. This result supports the mechanism of reconstructive transformation in solution involving a dissolution process followed by the CuO crystallization.

For the thermal dehydration of 1D $Cu(OH)_2$ nanostructures in the solid state, the $Cu(OH)_2$ nanowires obtained by the KOH/NH_3 route were selected as a representative example. After dehydration in the solid state at 120 °C for 2 h, bundles of CuO nanowires, which essentially reserved the morphology of the

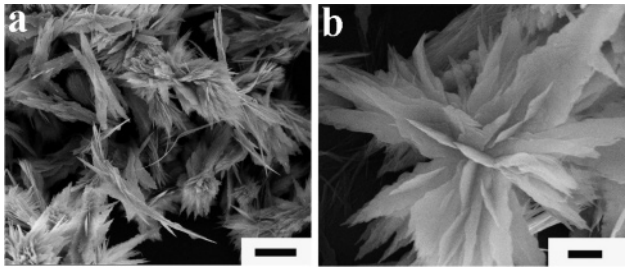

Figure 9. SEM images of CuO nanostructures obtained by thermal dehydration of the as-prepared $Cu(OH)_2$ nanoribbons in water at 70 °C for 12 h. Scale bars: (a) 2 μm; (b) 500 nm.

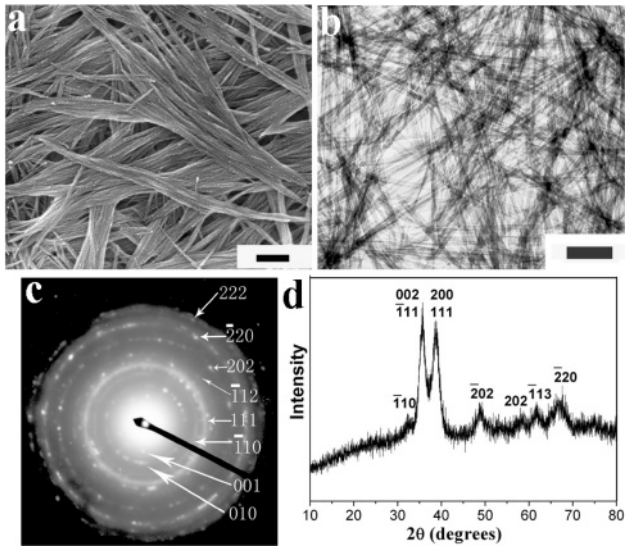

Figure 10. SEM (a) and TEM (b) images and ED (c) and XRD (d) patterns of CuO nanowires obtained by thermal dehydration of the as-prepared $Cu(OH)_2$ nanowires in the solid state at 120 °C for 2 h. Scale bars: (a) 500 nm; (b) 200 nm.

original $Cu(OH)_2$ nanowires, were obtained (Figure 10a,b). The related ED and XRD patterns demonstrate the complete conversion of $Cu(OH)_2$ to monoclinic CuO. The relatively broad peaks shown in the XRD pattern (Figure 10d) indicates that the CuO nanowires are actually polycrystalline nanowires consisting of primary nanocrystallites. This result suggests that the morphology of the 1D $Cu(OH)_2$ nanostructures obtained by the solution route can be well-reserved upon a simple heating process in the solid state, which is consistent with the result reported for the $Cu(OH)_2$ nanoribbons obtained by the surface oxidation of Cu and solution-phase coordination self-assembly.[12b]

Conclusions

In summary, a facile, template-free, low-temperature synthesis of $Cu(OH)_2$ nanowires and nanoribbons has been realized by simply dropping KOH and ammonia solutions into an aqueous $CuSO_4$ solution. According to the feeding order of the two alkaline solutions, the KOH/NH_3 route and the NH_3/KOH route were employed to selectively fabricate polycrystalline $Cu(OH)_2$ nanowires and single-crystalline $Cu(OH)_2$ nanoribbons, respectively. It has been reasonably proposed that the $Cu(OH)_2$ nanoribbons were formed by solution-phase coordination self-assembly at a relatively high $[Cu(NH_3)_n]^{2+}$ concentration, whereas the $Cu(OH)_2$ nanowires were formed by oriented attachment coupled with coordination self-assembly through a solid−solution−solid process, where a relatively low $[Cu(NH_3)_n]^{2+}$ concentration was retained. Ordered assemblies of $Cu(OH)_2$ nanorods were readily synthesized under the direction

of a polymeric additive in the solution. Furthermore, the transformation of the 1D $Cu(OH)_2$ nanostructures to well-defined CuO nanostructures, such as nanoplatelets, nanoleaflets, and nanowires, in the solution phase and in the solid state was investigated. It has been revealed that the conversion from $Cu(OH)_2$ to CuO in solution occurred mainly through a reconstructive transformation involving a dissolution process followed by the CuO crystallization, while the thermal dehydration of 1D $Cu(OH)_2$ nanostructures in the solid state normally resulted in the morphology-reserved 1D CuO nanostructures. The obtained low-dimenstion copper-based nanomaterials generally promise potential applications as sensors, catalysts, ferromagnets, and lithium ion electrode materials; moreover, the 1D $Cu(OH)_2$ nanostructures may have relevant biological implications due to their similarity in structure and morphology to the $Cu_2(OH)_3Cl$ nanofibers existing in living organisms as the first identified copper-based biomineral.[14] Finally, this simple route may provide an effective method for the morphological control of 1D nanostructures, and it is potentially extendable to other systems involving metal complexes with suitable combination of metals and ligands.

Acknowledgment. Financial support from NSFC (Grants 20325312, 20233010) and FANEDD (Grant 200020) is gratefully acknowledged.

References and Notes

(1) (a) Hu, J. T.; Odom, T. W.; Lieber, C. M. *Acc. Chem. Res.* **1999**, *32*, 435. (b) Patzke, G. R.; Krumeich, F.; Nesper, R. *Angew. Chem., Int. Ed.* **2002**, *41*, 2446. (c) Xia, Y.; Yang, P.; Sun, Y.; Wu, Y.; Mayers, B.; Gates, B.; Yin, Y.; Kim, F.; Yan, Y. *Adv. Mater.* **2003**, *15*, 353. (d) Rao, C. N. R.; Deepak, F. L.; Gundiah, G.; Govindaraj, A. *Prog. Solid State Chem.* **2003**, *31*, 5.

(2) (a) Sun, Y.; Mayers, B.; Herricks, T.; Xia, Y. *Nano Lett.* **2003**, *3*, 955. (b) Murphy, C. J.; Jana, N. R. *Adv. Mater.* **2002**, *14*, 80. (c) El-Sayed, M. A. *Acc. Chem. Res.* **2001**, *34*, 257.

(3) (a) Martin, C. R. *Science* **1994**, *266*, 1961. (b) Martin, B. R.; Dermody, D. J.; Reiss, B. D.; Fang, M.; Lyon, L. A.; Natan, M. J.; Mallouk, T. E. *Adv. Mater.* **1999**, *11*, 1021. (c) Huang, M. H.; Choudrey, A.; Yang, P. *Chem. Commun.* **2000**, 1063.

(4) (a) Braun, E.; Eichen, Y.; Sivan, U.; Ben-Yoseph, G. *Nature* **1998**, *391*, 775. (b) Reches, M.; Gazit, E. *Science* **2003**, *300*, 625. (c) Mao, C.; Solis, D. J.; Reiss, B. D.; Kottmann, S. T.; Sweeney, R. Y.; Hayhurst, A.; Georgiou, G.; Iverson, B.; Belcher, A. M. *Science* **2004**, *303*, 213.

(5) (a) Jana, N. R.; Gearheart, L.; Murphy, C. J. *Chem. Commun.* **2001**, 617. (b) Jana, N. R.; Gearheart, L.; Murphy, C. J. *J. Phys. Chem. B* **2001**, *105*, 4065.

(6) (a) Li, M.; Schnablegger, H.; Mann, S. *Nature* **1999**, *402*, 393. (b) Simmons, B. A.; Li, S.; John, V. T.; McPherson, G. L.; Bose, A.; Zhou, W.; He, J. *Nano Lett.* **2002**, *2*, 263. (c) Shi, H.; Qi, L.; Ma, J.; Cheng, H. *J. Am. Chem. Soc.* **2003**, *125*, 3450.

(7) (a) Peng, X.; Manna, L.; Yang, W.; Wickham, J.; Scher, E.; Kadavanich, A.; Alivisatos, A. P. *Nature* **2000**, *404*, 59. (b) Sun, Y.; Xia, Y. *Adv. Mater.* **2002**, *14*, 833. (c) Hu, J.-Q.; Chen, Q.; Xie, Z.-X.; Han, G.-B.; Wang, R.-H.; Ren, B.; Zhang, Y.; Yang, Z.-L.; Tian, Z.-Q. *Adv. Funct. Mater.* **2004**, *14*, 183. (d) Qi, L.; Cölfen, H.; Antonietti, M.; Li, M.; Hopwood, J. D.; Ashley, A. J.; Mann, S. *Chem. Eur. J.* **2001**, *7*, 3526. (e) Yu, S.-H.; Cölfen, H.; Antonietti, M. *Chem. Eur. J.* **2002**, *8*, 2937.

(8) (a) Gates, B.; Yin, Y.; Xia, Y. *J. Am. Chem. Soc.* **2000**, *122*, 12582. (b) Mayers, B.; Xia, Y. *Adv. Mater.* **2002**, *14*, 279.

(9) (a) Pan, Z. W.; Dai, Z. R.; Wang, Z. L. *Science* **2001**, *291*, 1947. (b) Kong, X. Y.; Ding, Y.; Yang, R.; Wang, Z. L. *Science* **2004**, *303*, 1348. (c) Ma, C.; Moore, D.; Li, J.; Wang, Z. L. *Adv. Mater.* **2003**, *15*, 228. (d) Dai, Z. R.; Pan, Z. W.; Wang, Z. L. *Adv. Funct. Mater.* **2003**, *13*, 9.

(10) (a) Sun, Y.; Mayers, B.; Xia, Y. *Nano Lett.* **2003**, *3*, 675. (b) Mo, M.; Zeng, J.; Liu, X.; Yu, W.; Zhang, S.; Qian, Y. *Adv. Mater.* **2002**, *14*, 1658.

(11) (a) Yu, S.-H.; Antonietti, M.; Cölfen, H.; Giersig, M. *Angew. Chem., Int. Ed.* **2002**, *41*, 2356. (b) Shi, H.; Qi, L.; Ma, J.; Cheng, H.; Zhu, B. *Adv. Mater.* **2003**, *15*, 1647.

(12) (a) Wen, X.; Zhang, W.; Yang, S.; Dai, Z. R.; Wang, Z. L. *Nano Lett.* **2002**, *2*, 1397. (b) Wen, X.; Zhang, W.; Yang, S. *Langmuir* **2003**, *19*, 5898.

(13) (a) Fujita, W.; Awaga, K. *J. Am. Chem. Soc.* **1997**, *119*, 4563. (b) Fujita, W.; Awaga, K. *Synth. Met.* **2001**, *122*, 569.

(14) (a) Lichtenegger, H. C.; Schoberl, T.; Bartl, M. H.; Waite, H.; Stucky, G. D. *Science* **2002**, *298*, 389. (b) Weiner, S.; Addadi, L. *Science* **2002**, *298*, 375.

(15) Zhu, C. L.; Chen, C. N.; Hao, L. Y.; Hu, Y.; Chen, Z. Y. *J. Cryst. Growth* **2004**, *263*, 473.

(16) Zhang, W.; Wen, X.; Yang, S.; Berta, Y.; Wang, Z. L. *Adv. Mater.* **2003**, *15*, 822.

(17) Wang, W.; Lan, C.; Li, Y.; Hong, K.; Wang, G. *Chem. Phys. Lett.* **2002**, *366*, 220.

(18) Song, X.; Sun, S.; Zhang, W.; Yu, H.; Fan, W. *J. Phys. Chem. B* **2004**, *108*, 5200.

(19) (a) Reitz, J. B.; Solomon, E. I. *J. Am. Chem. Soc.* **1998**, *120*, 11467. (b) Switzer, J. A.; Kothari, H. M.; Poizot, P.; Nakanishi, S.; Bohannan, E. W. *Nature* **2003**, *425*, 490.

(20) Chowdhuri, A.; Gupta, V.; Sreenivas, K.; Kumar, R.; Mozumdar, S.; Patanjali, P. K. *Appl. Phys. Lett.* **2004**, *84*, 1180.

(21) Gao, X. P.; Bao, J. L.; Pan, G. L.; Zhu, H. Y.; Huang, P. X.; Wu, F.; Song, D. Y. *J. Phys. Chem. B* **2004**, *108*, 5547.

(22) (a) Hsieh, C. T.; Chen, J. M.; Lin, H. H.; Shih, H. C. *Appl. Phys. Lett.* **2003**, *83*, 3383. (b) Chen, J.; Deng, S.; Xu, N.; Zhang, W.; Wen, X.; Yang, S. *Appl. Phys. Lett.* **2003**, *83*, 746.

(23) (a) Jiang, X.; Herricks, T.; Xia, Y. *Nano Lett.* **2002**, *2*, 1333. (b) Hsieh, C. T.; Chen, J. M.; Lin, H. H.; Shih, H. C. *Appl. Phys. Lett.* **2003**, *82*, 3316. (c) Wang, S. H.; Huang, Q. J.; Wen, X. G.; Li, X. Y.; Yang, S. H. *Phys. Chem. Chem. Phys.* **2002**, *4*, 3425.

(24) (a) Lee, S. H.; Her, Y. S.; Matijević, E. *J. Colloid Interface Sci.* **1997**, *186*, 193. (b) Cao, M.; Hu, C.; Wang, Y.; Guo, Y.; Guo, C.; Wang, E. *Chem. Commun.* **2003**, 1884. (c) Chang, Y.; Zeng, H. C. *Cryst. Growth Des.* **2004**, *4*, 397. (d) Liu, B.; Zeng, H. C. *J. Am. Chem. Soc.* **2004**, *126*, 8124.

(25) Wang, Z. L.; Kong, X. Y.; Wen, X.; Yang, S. *J. Phys. Chem. B* **2003**, *107*, 8275.

(26) (a) Penn, R. L.; Banfield, J. F. *Science* **1998**, *281*, 969. (b) Banfield, J. F.; Welch, S. A.; Zhang, H.; Ebert, T. T.; Penn, R. L. *Science* **2000**, *289*, 751. (c) Alivisatos, A. P. *Science* **2000**, *289*, 736. (d) Pacholski, C.; Kornowski, A.; Weller, H. *Angew. Chem., Int. Ed.* **2002**, *41*, 1188.

(27) Xu, G.; Yao, N.; Aksay, I. A.; Groves, J. T. *J. Am. Chem. Soc.* **1998**, *120*, 11977.

(28) Moulder, J. F.; Stickle, W. F.; Sobol, P. E.; Bomben, K. D. *Handbook of X-ray Photoelectron Spectroscopy*; Physical Electronics Division, Perkin-Elmer Corp.: Eden Prairie, MN, 1992.

(29) Laget, V.; Drillon, M.; Hornick, C.; Rabu, P.; Romero, F.; Turek, P.; Ziessel, R. *J. Alloys Compd.* **1997**, *262*−*263*, 423.

(30) Cudennec, Y.; Lecerf, A. *Solid State Sci.* **2003**, *5*, 1471.